Heliyon 9 (2023) e18299

Contents lists available at ScienceDirect

Heliyon

journal homepage: www.cell.com/heliyon

Antimicrobial and *in silico* studies of the triterpenoids of Dichapetalum albidum

Mary A. Chama [a,*], Godwin A. Dziwornu [a], Elizabeth Popli [b], Eduard Mas-Claret [c], Beverly Egyir [d], Daniel M. Ayine-Tora [a], Kofi B-A. Owusu [e], David G. Reid [b], Dorcas Osei-Safo [a], Melinda Duer [b], Dulcie Mulholland [f], Andreas Bender [b]

[a] *Department of Chemistry, SPMS, CBAS, University of Ghana, Ghana*
[b] *Yusuf Hamied Department of Chemistry, University of Cambridge, United Kingdom*
[c] *Royal Botanic Gardens, Kew, Richmond, TW9 3AQ, United Kingdom*
[d] *Department of Bacteriology, Noguchi Memorial Institute for Medical Research, College of Health Sciences, University of Ghana, Ghana*
[e] *Department of Parasitology, Noguchi Memorial Institute for Medical Research, College of Health Sciences, University of Ghana, Ghana*
[f] *Department of Chemistry, University of Surrey, Guildford, United Kingdom*

ARTICLE INFO

Keywords:
Dichapetalum albidum
2β, 6β, 21α-trihydroxyfriedelan-3-one
3β-acetoxy-2α,19β-dihydroxy-urs-12-en-28-oic acid
Leishmania donovani
Trypanosoma brucei brucei
Glucose-6-phosphate dehydrogenase

ABSTRACT

Here we report a new polyhydroxylated triterpene, 2β,6β,21α-trihydroxyfriedelan-3-one (**4**) isolated from the root and stem bark of *Dichapetalum albidum* A. Chev (Dichapetalaceae), along with six known triterpenoids (**1**–**3**, **5**, **6**, **8**), sitosterol-3β-*O*-D-glucopyranoside (**9**), a dipeptide (**7**), and a tyramine derivative of coumaric acid (**10**). Friedelan-3-one (**2**) showed an antimicrobial activity (IC_{50}) of 11.40 μg/mL against *Bacillus cereus*, while friedelan-3α-ol (**1**) gave an IC_{50} of 13.07 μg/mL against *Staphylococcus aureus* with ampicillin reference standard of 19.52 μg/mL and 0.30 μg/mL respectively. 3β-Acetyl tormentic acid (**5**) showed an IC_{50} of 12.50 μg/mL against *Trypanosoma brucei brucei* and sitosterol-3β-*O*-D-glucopyranoside (**9**) showed an IC_{50} of 5.06 μg/mL against *Leishmania donovani* with respective reference standards of IC_{50} 5.02 μg/mL for suramin and IC_{50} 0.27 μg/mL for amphotericin B. Molecular docking of the isolated compounds on the enzyme glucose-6-phosphate dehydrogenase (G6PDH) suggested 3β-acetyl tormentic acid (**5**) and sitosterol-3β-*O*-D-glucopyranoside (**9**) as plausible inhibitors of the enzyme in accordance with the experimental biological results observed.

1. Introduction

The increasing resistance to antibacterial drugs and the limited chemotherapy available against neglected tropical diseases are of global concern. In the search for new drugs, the molecular diversity afforded by natural products makes them attractive starting points in drug discovery ventures. Plants have a long history as sources of new drugs. Higher plants are sources for almost 25% of all pharmaceuticals [1]. Some drugs such as artemisinin and quinine were obtained directly from plants, while others were developed using plant-derived compounds as templates [2]. One approach to the discovery of new drugs is the analysis of medicinal plants as sources of new drug leads [3]. The first report of the dichapetalins and their potent cytotoxicity came from a study of *Dichapetalum madagascariense* (Dichapetalaceae) [4,5], which stimulated interest in the constituents of other species. This has led to the isolation of a

* Corresponding author.
E-mail address: machama@ug.edu.gh (M.A. Chama).

https://doi.org/10.1016/j.heliyon.2023.e18299
Received 20 February 2023; Received in revised form 7 July 2023; Accepted 13 July 2023
Available online 14 July 2023

total of 44 dichapetalins [6–11]. Nonetheless, investigations of other species, including *D. barteri* and *D. heudelotii* [10], have yielded no dichapetalins so far. Eighteen new dichapetalin-type triterpenoids called dichapegenins with four main structurally modified ring A have been isolated from *D. gelonioides*. Those with a phenyl-butadiene group include dichapegenins A–D. Dichapegenins E–L possess the phenyl-endoperoxide moiety. The phenyl-furan functionalized ring A include dichapegenins M – O whereas those with a phenyl-enedione motif are dichapegenins Q, R, and T [12].

The genus *Phyllanthus* (Euphorbiaceae) has also yielded structurally intriguing dichapetalin-type molecules, which possess diverse biological activities, especially toxicity against human tumor cells [13]. *Dichapetalum albidum* A.Chev. ex Pellegr (Family: Dichapetalaceae) is native to West Tropical Africa, including Ghana [14]. It is used locally as a pain killer during menstrual cycle and as emmenagogue. It is also used to treat chronic sores, urethritis, and rheumatism. With no prior phytochemical work documented, our present investigation sought to identify the potential antimicrobial constituents from *D. albidum* which can serve as potential drug leads. Herein, from the root and stem organic extracts, we report the isolation and characterization of a new polyhydroxylated triterpene, 2β,6β,21α-trihydroxyfriedelan-3-one (**4**) along with six known triterpenoids (**1**–**3**, **5**, **6**, **8**), a steroidal glycoside (Sitosterol-3β-*O*-D-glucopyranoside, **9**), a dipeptide (**7**), and a tyramine derivative of coumaric acid (**10**) (Fig. 1) and the antibacterial and antiparasitic activities. No dichapetalins were isolated.

2. Materials and methods

2.1. Plant collection, extraction, and isolation

D. albidum was collected from the Bobin Forest Reserve in the Ashanti Region of Ghana. A voucher specimen (DAD001) of the plant has been deposited at the Ghana Herbarium at the Department of Plant Science and Environmental Biology, University of Ghana. Each plant part (root and stem) was air-dried and pulverized. The root (450 g) and stem (1700 g) material were each extracted exhaustively and separately using a Soxhlet apparatus for 24 h with 4 L and 6 L of EtOAc, respectively. Dark green crude extracts of the root (8 g) and stem (30 g) were obtained after removal of the solvent *in vacuo*. Each crude extract was dissolved in a $(CH_3)_2CO$ – $CHCl_3$ mixture. Solids precipitated out, were filtered, and recrystallized from $(CH_3)_2CO$ to afford compound **1**, 200 mg (from the root extract) and 1400 mg (from the stem extract). The two supernatants were combined based on comparative TLC profiles and fractionated (34 g) on silica gel with Pet. ether/EtOAc (10:1, 10:3 and 10:6 v/v) to afford three fractions F1–F3. Fraction F1(11 g) was chromatographed on silica gel with Pet. ether/$CHCl_3$ (5:1, 5:2 and 5:3 v/v) to give five fractions F1A - F1E. Precipitates formed from fractions F1B–F1E were triturated with EtOH to afford the respective solids **2** (8 mg), **3** (14 mg), a mixture of stearic, behenic and lignoceric acids (85 mg), and compound **1** (108 mg). Fraction F2 (13 g) was chromatographed on silica gel with petroleum ether/EtOAc (10:1, 10:2 and 10:3 v/v) to give five fractions F2A-F2E. Solids that precipitated from fractions F2A and F2B were triturated (washed) with EtOH to afford compound **1** (15 mg) and a mixture of stigmasterol and β-sitosterol (186 mg), respectively. Fraction F2C was re-chromatographed with Pet. Ether/EtOAc (1:1–0:1 v/v) to afford F3A – F3C. Fraction F3A (g) was rechromatographed on silica gel with $CHCl_3$ to give five fractions coded $F3A_1$ – $F3A_5$. Precipitated solids from $F3A_1$ – $F3A_4$ were each triturated with different nonpolar solvents to afford **4** (11 mg), **5** (6 mg) and **7** (10 mg). Both fractions F3B and F3C were each triturated with EtOAc to afford **6** (8 mg), **8** (7 mg), **9** (25 mg) and **10** (7 mg).

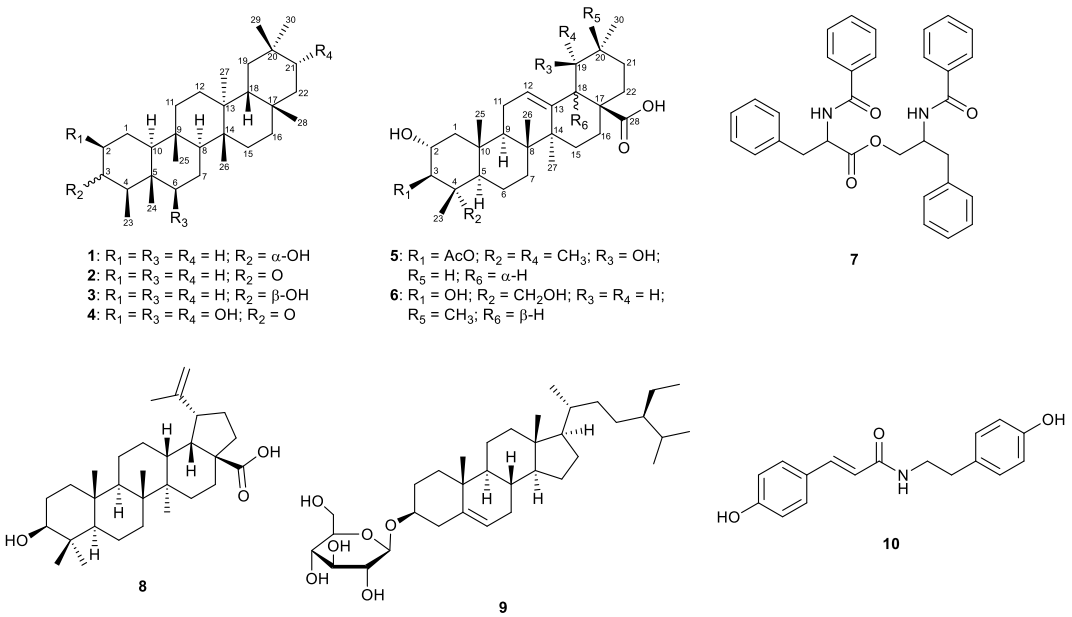

Fig. 1. Structures of compounds **1**–**10** from *D. albidum*.

2.2. General experimental procedure

Thin layer chromatography was performed on aluminum foil slides pre-coated with silica gel (thickness 0.2 mm, type Kieselgel 60 F_{254}, Merck, Rogers, AR); visualization of spots under UV light was done with UVGL-58 Handheld UV lamp at 254–365 nm. Compounds were also visualized by exposure to I_2 vapor or anisaldehyde spray reagent. Column chromatography was carried out on silica gel 60 (Fluka Analytical, Bellefonte, PA). Melting points (uncorrected) were determined on a Stuart Scientific Melting Point Apparatus (Sigma Aldrich, St. Louis, MO). Infrared (IR) spectra were obtained on a PerkinElmer Spectrum 100 spectrometer equipped with an Attenuated Total Reflection (ATR) sampling accessory. Abbreviations for IR bands are strong (s), medium (m), weak (w) and broad (b).

2.2.1. Nuclear Magnetic Resonance

Solution state NMR of pure isolates were run on a 500, 600 or 700 MHz Brüker Avance instrument at 125, 150 or 175.5 MHz for ^{13}C NMR and 500, 600 or 700 MHz for ^{1}H NMR respectively. Depending on the solubility of a particular compound, solvents used were $CDCl_3$, CD_3OD, DMSO-d_6, or acetone-d6 with TMS as the internal standard. The coupling constants *J* are given in Hz. Compounds were dissolved in the minimum amount of cold, deuterated solvent. Most of the solution-state NMR spectra were acquired at the Cambridge Chemical Laboratory NMR service of the Yusuf Hamied Department of Chemistry, University of Cambridge, United Kingdom.

2.2.2. High resolution mass spectrometry

Mass Spectrometry was carried out at the Chemical Laboratory Mass Specrometry service of the Yusuf Hamied Department of Chemistry, University of Cambridge, United Kingdom on a Waters Xevo G2-XS QT Quadrupole Time-of-Flight Mass Spectrometer. ASAP+ and ASAP- experiments were run between 50 and 2500 Da using the following tuning parameters: corona current 3.0; probe

Table 1
NMR spectroscopic data for compounds **4** (^{1}H, 400 MHz and^{13}C, 100 MHz, $CDCl_3$) and **5** (^{1}H, 700 MHz and^{13}C, 175 MHz, Acetone-d_6) (*J* in Hz).

Position	4 ($CDCl_3$)		5 ($(CD_3)_2CO$)	
	δ_C ppm	δ_H ppm	δ_C ppm	δ_H ppm
1	32.3	2.45 m	48.4	1.97 m
		1.58 m		1.02 m
2	74.9	4.09 ddd (14.2, 3.4, 0.9)	66.7	3.77 b ($W_{1/2}$ = 13.0)
3	212.3	–	85.1	4.50 d (9.9)
4	55.8	2.45 q (4.0)	39.9	–
5	48.4	–	55.9	1.00 m
6	79.6	3.66 dd (10.3, 4.6)	19.2	1.54 m
				1.43 dd (12.6, 3.0)
7	29.6	1.68 m	33.7	1.60 m
		1.42 m		1.32 ddd (13.0, 3.1, 3.1)
8	48.6	1.50 dd (13.0, 3.7)	40.7	–
9	37.5	–	48.0	1.80 dd (10.9, 6.9)
10	55.7	1.52 m	38.7	–
11	35.3	1.48 m	24.4	2.02 m
		1.28 m		1.98 m
12	30.2	1.42 m	128.6	5.29 dd (3.6, 3.6)
		1.31 m		
13	39.2	–	139.8	–
14	38.8	–	42.3	–
15	30.6	1.43 m	29.3	1.83 td (13.7, 4.7)
		1.32 m		0.99 ddd (13.7, 4.4, 2.2)
16	36.1	1.57 m	26.4	2.63 td (13.3, 4.7)
				1.52 ddd (13.3, 4.7, 2.4)
17	32.6	–	48.3	–
18	44.4	1.52 m	54.5	2.55 s
19	36.1	1.64 dd (12.7, 3.4)	73.3	–
		1.50 dd (13.0, 3.7)		
20	34.5	–	42.6	1.38 m
21	74.4	3.69 dd (11.9, 3.6)	27.0	1.75 m
				1.22 ddd (12.9, 7.1, 3.4)
22	47.1	1.71 dd (12.3, 12.3)	38.5	1.74 dd (10.2, 3.0)
		1.24 dd (12.9, 3.9)		1.65 dd (13.7, 4.3)
23	10.1	1.21 d (6.7)	29.1	0.85 s
24	9.4	0.74 s	18.2	0.86 s
25	18.1	0.86 s	17.0	1.01 s
26	17.7	0.90 s	17.4	0.78 s
27	19.4	1.11 s	24.7	1.36 s
28	33.3	1.20 s	179.2	–
29	25.0	0.99 s	27.3	1.21 s
30	32.0	1.07 s	16.6	0.94 d (6.7)
3-OAc			171.3	–
			21.1	2.02 s

temperature 40 °C; sampling cone 30.0000; source temperature 120 °C; source offset 80; cone gas flow 50.0 L/Hr; and desolvation gas flow 500.0 L/Hr. Samples were referenced against sodium iodide.

2.2.3. X-ray analysis

X-Ray analysis was performed at the University of Cambridge X-Ray Crystallography service of the Yusuf Hamied Department of Chemistry, University of Cambridge, United Kingdom for compounds **1** and **3**. Where possible, solvent was slowly evaporated from a saturated solution of compounds, at room temperature, to grow crystals large enough for single crystal X-Ray Diffraction (XRD). Bond lengths/angles, unit cell dimension and packing parameters were determined. Structures were analyzed and displayed using the Mercury program of the Cambridge Crystallographic Data Centre (CCDC, 2017).

2.3. Physicochemical data of isolated compounds

2β,6β,21α-Trihydroxyfriedelan-3-one, (**4**): (11 mg): white powder; mp. 262–264 °C(Me_2CO); $R_f = 0.88$ (Pet. Ether/EtOAc, 1:4 v/v); ^1H and ^{13}C NMR data (Table 1); HR-ESI-MS: *m/z* 475.3785 $[M+H]^+$ (calcd for 475.3787, $C_{30}H_{51}O_4$).

3β-Acetyl tormentic acid (**5**): (6 mg): white powder; mp. 224–226 °C (Hexane); $R_f = 0.95$ (Pet. Ether/EtOAc 7:3 v/v); ^1H and ^{13}C NMR data (Table 1); HR-ESI-MS: *m/z* 553.3497 $[M+Na]^+$ (calcd for 553.3499, $C_{32}H_{50}O_6Na$).

2.4. Biological methods

2.4.1. Antibacterial activity

Staphylococcus aureus (ATCC 29213), *Bacillus cereus* (ATCC 14579), and *Escherichia coli* (ATCC 25922) were used in the current study. Bacteria species were plated on Mueller-Hinton agar (Sigma-Aldrich, USA) and incubated overnight at 37 °C. Selected three colonies of each bacteria were incubated overnight at 37 °C for bacteria to reach the log phase of growth. Stock solutions of each of compounds **1**, **2**, **5**, **6**, **7**, **9** were prepared at a concentration of 10 mg/mL in dimethyl sulfoxide. The compound solutions were vortexed, and filter sterilized into vials through 0.45 μm Millipore filters under sterile conditions and stored at −20 °C until use. The antibacterial activities of compounds **1, 2, 5, 6, 7, 9** were assessed by slight modification of the Alamar Blue assay (Life Technologies, USA) to determine the Inhibitory Concentrations as described in reference [15]. The log phases of the three bacteria were diluted with sterile saline to achieve a turbidity of 0.5 McFarland standard of an approximate concentration of 2×10^8 CFU/mL. Each bacterial strain was then diluted to its working concentration. Log phase of bacteria at a concentration range of 1×10^2 to 1×10^6 CFU/mL were incubated with different concentrations of compounds (0–100 μg/mL), and 10% Alamar Blue® reagent at 37 °C for 6–8 h. Absorbance was read at 540 nm with a reference wavelength of 595 nm, and half maximal inhibitory concentration (IC_{50}) values of compounds were calculated by the plot of a growth curve. Ampicillin was used as positive control for the standard bacteria.

2.4.2. Antitrypanosomal activity

The GUTat 3.1 bloodstream form of *Trypanosoma brucei brucei* parasites was used to assess the antitrypanosomal activity of compounds **1**, **2**, **5**, **6**, **7**, **9**. *In vitro* cultured parasites at established conditions [16] were used at a confluent concentration of 1×10^6 parasites/mL and the Neubauer counting chamber was used to estimate the parasitemia. HM1-9 medium was used to dilute parasites to a concentration of 3×10^5 parasites/mL for successive experiments. The Alamar Blue assay was used for viability test on the trypanosome parasites based on similar methods to the manufacturer's [16] in a 96-well plate. Parasite concentration of 3×10^5 parasites/mL were seeded with varying concentrations of the compounds from 0 μg/mL to 100 μg/mL. Final concentrations of DMSO were kept at less than 0.1%. After incubation of parasites with or without the compounds for 24 h at 37 °C in 5% CO_2, 10% Alamar Blue dye was added to the parasites and incubated for another 24 h in the dark. Suramin (Sigma-Aldrich, USA) was used as a positive control standard. After a total of 48 h, absorbance was read at 540 nm using a spectrophotometer (TECAN Sunrise Wako, AUSTRIA GmbH). Trend curves were drawn to obtain the 50% inhibitory concentration (IC_{50}) of each compound using GraphPad Prism (v.7).

2.4.3. Antileishmanial activity

Promastigote forms of *L. donovani* (D10) cultures were used in this study. Parasites were cultured *in vitro* according to conditions established [16] with slight modifications. Parasite concentration of 1×10^6 parasites/mL was diluted to a parasitemia of 3×10^5 parasites/mL with M − 199 medium supplemented with 10% heat inactivated FBS, gentamycin, and BME vitamins before being used for subsequent experiments. Estimation of parasite concentration was done with the Neubauer counting chamber. The Alamar Blue cell viability assay was performed on the *L. donovani* promastigote forms according to the manufacturers protocol with slight modifications [16]. The promastigotes were seeded at cell density of 3×10^6 cells/mL in 96-well plates and incubated for 48 h at 28 °C with or without the compounds at concentrations of 0–100 μg/mL. Final concentrations of DMSO were kept below 0.1%. Amphotericin B was used as the reference drug. Ten percent of Alamar Blue reagent was added 4 h prior to the end of treatment and absorbance was read at 540 nm using a microtiter-plate reader (TECAN Sunrise Wako, AUSTRIA GmbH). Trend curves were drawn to obtain the 50% inhibitory concentration (IC_{50}) of each compound using GraphPad Prism (v.7).

2.5. Molecular docking studies

To determine which targets are likely to bind to the isolated compounds tested for the protozoan parasites, *T. b. brucei* and

L. donovani, a literature search was carried out which identified the enzyme, glucose-6-phosphate dehydrogenase (G6PDH). The enzyme is a ubiquitous enzyme that catalyses the first and rate-limiting step of the pentose phosphate pathway (PPP). This enzyme catalyses the oxidation of glucose-6-phosphate (G6P) into 6-phospho-gluconolactone, which produces ribose 5-phosphate (R5P), a precursor of nucleic acid synthesis. Aside from the metabolic role, G6PDH also provides the cell with NADPH for biosynthetic processes as well as protects cell against oxidative stress [17–20]. G6PDH has been shown to be important for the survival of protozoan parasites, which makes this enzyme an attractive target for drugs against parasitic protozoans such as *T. b. brucei* [21] and *L. donovani*. The most active known inhibitors of TcG6PDH are steroids [22–25]. This makes the steroids promising leads for the development of new parasite-selective chemotherapeutic agents. Some of these steroids have been shown to kill cultured trypanosomes but not Leishmania [21]. For this reason, the ten identified compounds from *D. albidum*, friedelan-3α-ol (**1**), friedelan-3-one (**2**), friedelan-3β-ol (**3**), 2β,6β, 12α-trihydroxyfriedelane-3-one (**4**), 3β-acetyl tormentic acid (**5**), arjunolic acid (**6**), *N*-benzoylphenylalaninyl-*N*-benzoylphenylalaninate (**7**), betulinic acid (**8**), sitosterol-3β-*O*-D-glucopyranoside (**9**)-a eukaryotic DNA polymerase lambda inhibitor, and *N-trans*--*p*-coumaroyltyramine (**10**) were docked to the crystal structure of the TcG6PDH (PDB ID: 5AQ1, resolution 2.65 Å) [26] which was obtained from the Protein Data Bank (PDB) [27,28]. The Scigress program (version FJ 2.6) [29] was used to prepare the crystal structure for docking, in which hydrogen atoms were added and the co-crystallized ligand G6P and NAPH were removed. The centre of the binding pocket was defined as the oxygen in the ring of G6P (x = 79.171, y = 119.883, z = 69.7) with a radius of 10 Å. The GoldScore (GS) [30], ChemScore (CS) [31,32], ChemPLP [33] and Astex Statistical Potential (ASP) [34] scoring functions were implemented to validate the predicted binding modes and relative energies of the ligands using the GOLD v5.4 software suite. The co-crystallized ligand (G6P) was first docked, and root mean square deviation (RMSD) values were calculated for the heavy atoms. The average RMSD obtained for ASP was 0.769, while those obtained for PLP was 0.581, CS and GS were respectively 0.615 and 0.442, indicating the strong prediction power of the scoring functions. The binding scores obtained are presented in Table 3 whiles the RMSD values are in supplementary information S3. The QikProp 3.2 [35] software package was used to calculate the molecular descriptors (MW, HBD, HBA, PSA, LogP, and RB) of compounds **1**–**10**.

3. Results and discussion

3.1. Identification of isolated compounds

Compounds **1**, **2** and **3** were separately isolated as white amorphous solids. They exhibited typical oleanane-type triterpenoids from their ^{1}H and ^{13}C NMR spectra.

Compounds **1** and **3** gave the same HR-ESI-MS value of 425.3770 (calculated for 425.3783 $[M+H]^+$, $C_{30}H_{51}O$), two (2) units higher than compound **2**. Comparison of their NMR spectra with literature indicated that compounds **1** and **3** were friedelins [36,37]. Minor noticeable differences were observed in the C-3 chemical shifts and the $W_{1/2}$ value of H-3. Because of the observation of only one point of difference from NMR data of compounds **1** and **3**, single crystal X-ray diffraction analyses of **1** and **3** (Supplementary Information S2) was undertaken to confirm their structures as friedelan-3α-ol and friedelan-3β-ol, respectively. Compound **2** showed a ketone carbonyl carbon signal at δ_c 213.4 ppm, indicating an oxidation of the C-3 hydroxy group of compounds **1** and **3**. Comparison of the NMR data with literature [38] confirmed **2** as friedelan-3-one. The friedelanes are common in most plants, including *Dichapetalum* species [6,9, 39]. However, the occurrence of friedelan-3α-ol is rare and reported herein for the first time from a *Dichapetalum* species.

Compound **4** gave a $[M+H]^+$ ion at m/z 475.3785 (calcd for 475.3787, $C_{30}H_{51}O_4$) in HR-ESI-MS, consistent with a molecular formula of $C_{30}H_{50}O_4$. It showed characteristic oleanane NMR spectra similar to those of compounds **1**–**3**. Unlike **1** and **3**, there were three hydroxyl groups in compound **4** occurring at C-2, C-6, and C-21. The ^{13}C NMR spectra of **4** showed characteristic oxymethine signals at δ_c 74.9, 79.6, and 94.4 ppm for C-2, C-6 and C-21 respectively (Fig. 1 and Table 1). C-3 occurred as a carbonyl signal at δ_c 212.3 ppm. Use was made of HMBC and COSY experiments to determine the structure of **4** (Fig. 2A), and the NOESY spectrum was used to assign the relative stereochemistry at key chiral centers (Fig. 2B). Six coupled spin systems were observed in the COSY spectrum (Fig. 2A).

Key HMBC correlations were observed from both H-1 and H-23 to the C-3 carbonyl carbon, while the H-4 resonance correlated with the oxymethine C-2 and C-6 carbons. The position of the hydroxyl group in ring E was established through COSY correlations seen between H-21 and with both H-22 and HMBC correlations between the methyl protons 3H-29 and 3H-30 and C-21. In the NOESY

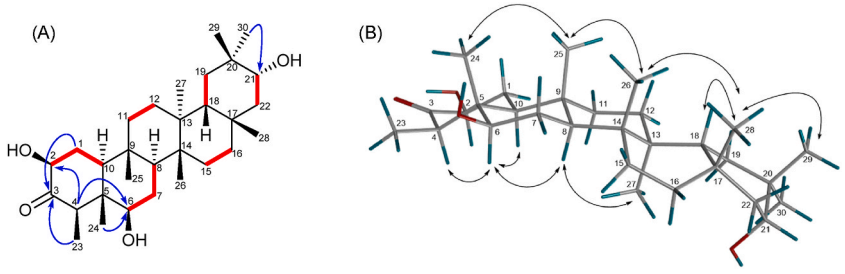

Fig. 2. (A): Key COSY (red bold bonds) and HMBC (blue arrows) correlations(B): NOESY (double headed arrows) correlations observed for compound 4. (For interpretation of the references to colour in this figure legend, the reader is referred to the Web version of this article.)

spectrum, based on cross correlations between the methine protons of H-4, H-8, and H-10 with H-2 and H-6, the hydroxyl groups at C-2 and C-6 were relatively assigned the β configuration. NOESY correlations between H-18, 3H-26, 3H-28, with H-21 suggested the latter could be assigned as β. As a result, the configuration of the hydroxy group at C-21 was assigned as α, as previously observed with related friedelanes [40]. Thus, the structure of **4** was elucidated as 2β,6β,21α-trihydroxyfriedelan-3-one and is reported here for the first time.

An analysis of the 1D NMR spectra of compound **5** indicated a pentacyclic-type triterpene. The HSQC spectrum showed the presence of eight methyl groups, including an acetoxy group (δ_c 21.1) at C-3 (Table 1 and Fig. 3). Eight methylenes, seven methines of which two are oxymethines with resonances at δ_c 66.7 (C-2) and δ_c 85.1 (C-3), and one tri-substituted olefinic double bond carbon resonance at δ_c 128.6 (C-12), were also observed. The presence of nine quaternary carbon signals observed included two carbonyls due to a carboxylic acid (δ_c 171.3, C-28) and an acetoxy group on C-3 (δ_c 179.2), a tri-substituted olefinic double bond carbon resonance (δ_c 139.8, C-13), and an oxygenated quaternary carbon (δ_c 73.3, C-19). The presence of two methyls, 3H-29 (δ_H 1.21, s) and 3H-30 (δ_H 0.94, d, $J = 6.7$), with corresponding ^{13}C resonances at δ_c 73.3 and δ_c 42.6 respectively, together with the two-singlet gem-dimethyls at δ_H 0.85 (3H-23) and 0.86 (3H-24) on C-4 (δ_C 39.9) were indicative of an ursane triterpene skeleton. The HR-ESI-MS data (*m/z* 553.3497 $[M + Na]^+$, calcd. 553.3499) obtained for compound **5** was consistent with a molecular formula of $C_{32}H_{50}O_6$, corroborating eight degrees of unsaturation.

Information from the analyses of ^1H NMR, ^1H–^1H–COSY and HSQC spectra also identified five ABX coupling systems at δ_H 3.77 (bs, $W_{1/2} = 13.0$, H-2), 1.97 (m, H-1a), and 1.02 (m, H-1b); δ_H 1.00 (m, H-5), 1.43 (dd, $J = 12.6, 3.0$, H-6a), and 1.54 (m, H-6b); δ_H 1.80 (dd, $J = 10.9, 6.9$, H-9), 2.02 (m, H-11a), and 1.98 (m, H-11b); δ_H 5.29 (dd, $J = 3.6, 3.6$, H-12), 2.02 (m, H-11a), and 1.98 (m, H-11b); and finally, δ_H 1.38 (m, H-20), 1.75 (m, H-21a) and 1.22 (ddd, $J = 12.9, 7.1, 3.4$, H-21b) (Fig. 3A). The relative stereochemistry of H-2 was supported by correlations with the methyl protons 3H-24 and 3H-25 in the NOESY spectrum (Fig. 3B). Similarly, NOESY correlations between H-3, H-5, H-9, and H-23 confirmed these were placed at the same side of the molecule. Significantly, the methyl protons 3H-27, 3H-29, and 3H-30 showed correlations in the NOESY spectrum with the methine proton H-18, suggesting an alpha orientation of 19-OH. Compound **5** was found to be identical with 3β-acetyl tormentic acid [41,42] previously isolated from *Cecropia lyratiloba* [40], even though there were some NMR misassignments which have been corrected in this work. These include H-5 (δ_H 1.00, previously reported as δ_H 5.20), C-20 (δ_C 42.6, previously reported as δ_C 54.4), C-22 (δ_C 38.5, previously reported as δ_C 32.4) and 3-OAc (CH_3 δ_C 21.1, previously reported as δ_C 53.3). All other resonances were consistent with those reported by Tane et al. [40]. The spectral data of compound **5** was also consistent with 3β-acetyl tormentic acid semi synthesized from monoacetylation of tormentic acid [42].

The NMR spectra of **6** were comparable to compounds **4** and **5,** with a carboxylic acid at C-28 (δ_C 182.1), two hydroxymethine carbons at C-2 (δ_C 69.8) and C-3 (δ_C 78.2), a C-23 hydroxymethylene carbon (δ_C 66.3), and a trisubstituted double bond between C-12 (δ_c 123.5) and C-13 (δ_c 145.5). The compound was identified as the known arjunolic acid [43]. Compound **7** was identified as *N*-benzoyl-L-phenylalaninyl-*N*-benzoyl-L-phenylalaninate, known commonly as asperphenamate or auranamide, after comparison with literature spectral data, as well as HR-ESI-MS results [44] (Supplementary Information S1). Formed from the condensation of *N*-benzoyl-L-phenylalanine and N-benzoyl-L-phenylalaninol, compound **7** has been reported from plants harboring endophytic fungi [45] and is reported here for the first time from *Dichapetalum*. The dipeptide aurantiamide acetate, which has similar structure to *N*-benzoylphenylalaninyl-*N*-benzoylphenylalaninate has been isolated previously from *D. pallidum* [10]. Compound **8** was identified as betulinic acid based on comparison of spectral data from that isolated from *D. barteri* [46]. Even though most *Dichapetalum* species are known for their dichapetalin-type triterpenoids, no such compounds were isolated from *D. albidum*, as also not observed from species such as *D. barteri* [46] and *D. heudelotii* [10].

Compound **9** showed a part of an NMR spectra that was similar to a triterpenoid and a part attributed to glycoside. Comparison of literature data with those of spectra of compound **9**, identified it as a sitosterol-3β-*O*-D-glucopyranoside. Nevertheless, varied classes of compounds such as oleananes, ursane, lupanes, steroidal glycoside (sitosterol-3β-*O*-D-glucopyranoside, 9), a tyramine derivative of coumaric acid and a dipeptide (*N-trans-p*-coumaroyl tyramine, 10) were present.

3.2. Biological activity

Six of the isolated compounds (**1**, **2**, **5**, **6**, **7** and **9**) were tested against the three bacterial strains, *Escherichia coli* (ATCC 25922),

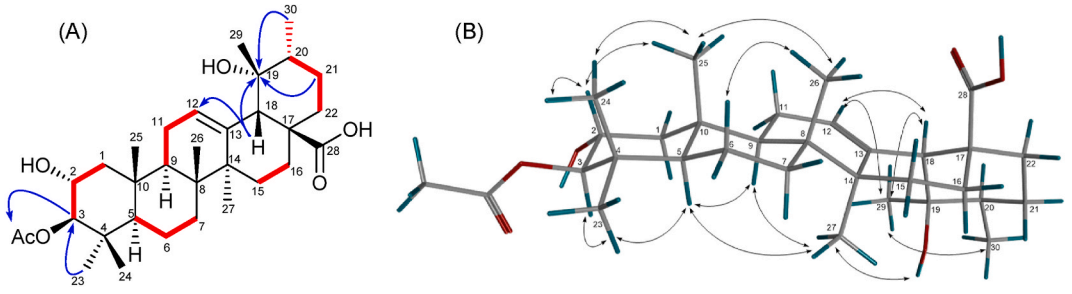

Fig. 3. (A): Key COSY (red bold bonds) and HMBC (blue arrows) correlations(B): NOESY (double headed arrows) correlations observed for compound 5. (For interpretation of the references to colour in this figure legend, the reader is referred to the Web version of this article.)

Staphylococcus aureus (ATCC 29213) and *Bacillus cereus* (ATCC 14579), as well as the parasites *L. donovani* and *T. b. brucei* (Table 2). Among them, friedelan-3-one (**2**) was active against all the three bacterial strains with the most activity observed against *B. cereus* (IC_{50} = 11.40 μg/mL), and being more active than the standard ampicillin (19.52 μg/mL). Friedelan-3α-ol (**1**) was more selective against *S. aureus* (IC_{50}, 13.07 μg/mL). Similarly, compounds **5** and **7** showed better selectivity against *E. coli* and *B. cereus*, respectively. Arjunolic acid (**6**) did not show activity against any of the three tested bacteria strains. Compound **5** was the most active (12.50 μg/mL) against *T. b. brucei*, while arjunolic acid (**6**) and *N*-benzoylphenylalaninyl-*N*-benzoylphenylalaninate (**7**) showed about two-fold better activities (IC_{50}, 28.49 and 33.28 μg/mL respectively) compared to friedelan-3α-ol (**1**) and friedelan-3-one (**2**). Sitosterol-3β-*O*-D-glucopyranoside (**9**) showed a good activity against *L. donovani* (IC_{50}, 5.06 μg/mL) compared to the standard amphotericin B which had a value of 0.27 μg/mL.

Friedelan-3α-ol **(1);** friedelan-3-one **(2);** 3β-acetyl tormentic acid (**5);** arjunolic acid (**6**); *N*-benzoylphenylalaninyl-*N*-benzoyl-phenylalaninate (**7);** sitosterol-3β-*O*-D-glucopyranoside (**9**).

Friedelan-3-one isolated from *D. crassifolium* was less active with IC_{50} of 378.10 μg/mL against *S. haematobium* eggs compared with praziquantel standard (15.47 μg/mL) [39]. From *D. madagascariense*, it showed activity of 0.95 μg/mL against the hookworm, *Necator americanus* whiles the most potent was friedelan-3β-ol (0.64 μg/mL) and a mixture of the two, gave a reduced activity of 1.72 μg/mL compared to albendazole (0.0024 μg/mL, [47]. Antimicrobial activities have also been reported for both friedelan-3-one and friedelan-3β-ol isolated from different plant extracts. Friedelan-3-one has showed antifungal activity against *C. albicans* with a zone of inhibition of 11 mm at 100 μg/mL [48]. Friedelan-3-one isolated from *Pterocarpus santalinoides* has showed antibacterial activities against different bacterial species including *Staphylococcus aureus, Corynebacterium ulcerans, Streptococcus pneumoniae* [49].

3.3. Molecular docking results

The molecular docking results of the ten compounds; friedelan-3α-ol (**1**), friedelan-3-one (**2**), friedelan-3β-ol (**3**), 2β,6β,12α, trihydroxyfriedelane-3-one (**4**), 3β-acetyl tormentic acid (**5**), arjunolic acid (**6**), N-benzoylphenylalaninyl-N-benzoylphenylalaninate (**7**), betulinic acid (**8**), sitosterol-3β-*O*-D-glucopyranoside (**9**), and *N-trans-p*-coumaroyl tyramine (**10**) are showed in Table 3. The scoring functions of the isolated compounds were compared with the known ligands; 16-bromodehydroepiandrosterone (16BrDHEA), 16-bromoepiandrosterone (16BrEA), cholesterol, dehydroepiandrosterone (DHEA), and epiandrosterone (EA) [22,23,25,26].

The compounds were docked at the binding pocket of TcG6PDH which comprised of hydrophilic and lipophilic sections. The modelling shows that the compounds occupied the binding pockets with plausible binding modes. Therefore, they are favorably disposed towards the binding sites of the enzyme with no strain and the lipophilic moieties are not pointing towards the aqueous environments. The most active compounds formed hydrogen bonds to Glu285, Arg408, Lys251, His241, Tyr248 and Gln437. The modelling for sitosterol-3β-*O*-D-glucopyranoside (**9**) shows that the main contribution to the energy of binding is made by hydrogen bonds present between the hydroxy groups of the glucose moiety and Glu285, His241, Arg408 and Lys251 as shown in Fig. 4 (**A**, **B**). For 3β-acetyl tormentic acid **(5)**, 2-OH also forms a hydrogen bond with the side chain carboxylic acid moiety of Glu285 and the carbonyl group of 3-AcO forms hydrogen bonds with Gln437 and Tyr248, as shown in the docked configuration in Fig. 5 (**A**, **B**). Considering the binding affinities, sitosterol-3β-*O*-D-glucopyranoside (**9**) and 3β-acetyl tormentic acid (**5**), which are the most active molecules against *L. donovani* and *T. b. brucei* respectively, also had the highest scores compared to the known inhibitors (Table 3).

(**A**): The ligand occupies the binding pocket. The protein surface is rendered. Brown depicts hydrophobic regions on the surface while blue depicts hydrophilic areas. (B): Hydrogen bonds are shown as green line between 3β-acetyl tormentic acid and the amino acid Glu285, Gln437, Tyr248 and Glu216.

3.3.1. Chemical space

The calculated molecular descriptors of the docked compounds, molecular weight (MW), log*P*, Hydrogen bond donor (HBD), Hydrogen bond acceptor (HBA), Polar Surface Area (PSA) and Rotatable Bonds (RB) are given in Table 4. The HBDs for these molecules are within the lead-like chemical space, the MW and RB are in the drug-like chemical space and log *P* is in a known drug recognition region. For definition of lead-like, drug-like and Known Drug Space regions [50] see Table S3 in the Supplementary Information. These values demonstrate that the molecules can be optimized as drug leads for further drug development.

Due to paucity of the compounds isolated, the study could not carry out an experimental validation of the predicted targets.

Table 2
Antibacterial and anti-parasitic activities (IC_{50}, μg/mL) of some compounds isolated from *D. albidum*.

Compound/IC_{50} (μg/mL)	*E. coli*	*S. aureus*	*B. cereus*	*L. donovani*	*T. b. brucei*
1	99.65	13.07	97.76	>100	51.60
2	70.26	54.76	11.40	>100	53.47
5	29.86	>100	>100	>100	12.50
6	>100	>100	>100	>100	28.49
7	>100	>100	49.26	>100	33.28
9	>100	>100	>100	5.06	>100
Ampicillin	8.97	0.30	19.52		
Amphotericin B				0.27	
Suramin					5.02

Table 3
Results of the scoring function for the co-crystalised, the isolated compounds and literature ligands docked with the glucose-6-phosphate dehydrogenase (G6PDH).

COMPOUND	ASP	Chem PLP	Chem Score	Gold Score
FRIEDELIN-3α-OL (1)	18.01	53.90	27.75	44.95
FRIEDELAN-3-ONE (2)	20.30	43.10	29.40	45.70
FRIEDELIN-3β-OL (3)	18.63	41.44	28.31	43.85
2β,6β,21α-TRIHYDROXYFRIEDELAN-3-ONE (4)	21.20	49.10	29.20	41.10
3β-ACETYL TORMENTIC ACID (5)	25.50	50.08	26.08	45.90
ARJUNOLIC ACID (6)	25.10	48.50	24.60	49.70
***N*-BENZOYL-L-PHENYLALANINYL-*N*-BENZOYL-L-PHENYLALANINATE** (7)	37.75	79.79	35.09	67.01
BETULINIC ACID (8)	21.50	51.00	29.80	46.00
SITOSTEROL-3β-*O*-D-GLUCOPYRANOSIDE (9)	35.30	70.80	32.10	67.40
***N-TRANS-P*-COUMAROYLTYRAMINE** (10)	27.20	54.20	24.40	49.50
KNOWN LIGANDS				
GLUCOSE 6-PHOSPHATE (G6P)	26.50	53.30	21.60	70.10
16-BROMODEHYDROEPIANDROSTERONE (16BRDHEA)	21.20	48.10	24.60	41.60
16-BROMOEPIANDROSTERONE (16BREA)	22.40	51.00	23.80	41.90
CHOLESTEROL	28.40	56.70	29.70	45.80
DEHYDROEPIANDROSTERONE (DHEA)	20.80	43.10	24.00	36.10
EPIANDROSTERONE (EA)	21.00	46.10	24.10	38.10

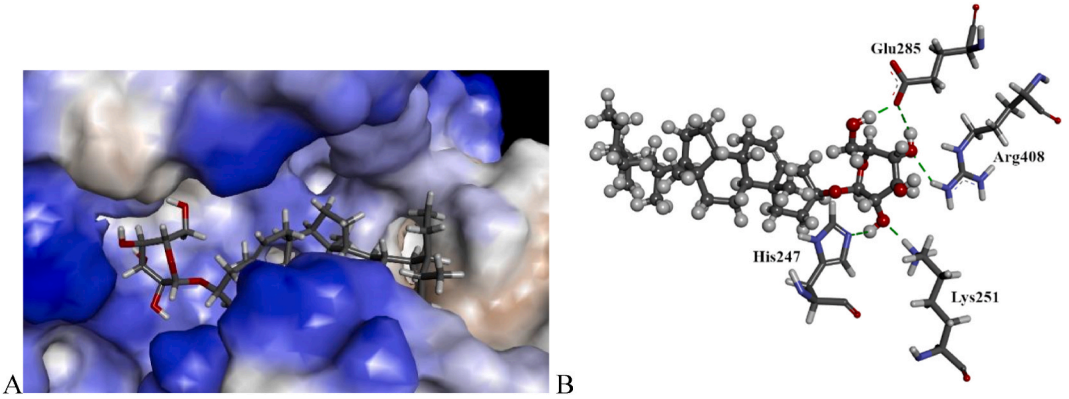

Fig. 4. The docked configuration of sitosterol-3β-*O*-D-glucopyranoside (**9**), in the binding site of G6PDH as predicted by GoldScore. (A): The ligand occupies the binding pocket. The protein surface is rendered. Brown depicts hydrophobic regions on the surface while blue depicts hydrophilic areas. (**B**): Hydrogen bonds are shown as green lines between sitosterol-3β-*O*-D-glucopyranoside and the amino acids Lys251, Glu285, Arg408 and His247. (For interpretation of the references to colour in this figure legend, the reader is referred to the Web version of this article.)

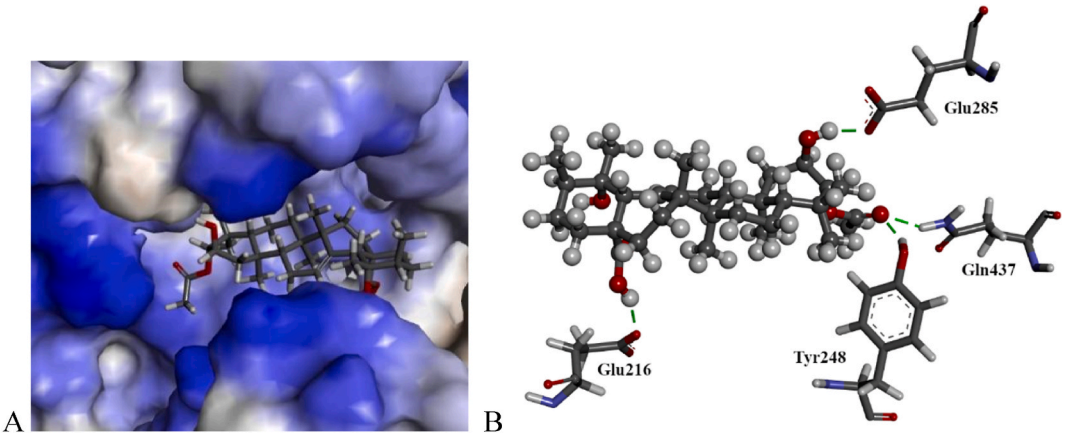

Fig. 5. The docked configuration of 3β-acetyl tormentic acid (**5**), in the binding site of G6PDH as predicted by ChemScore.

Table 4
The calculated molecular descriptors for the ligands of *D. albidum*.

Ligand	MW	HBD	HBA	LogP	PSA	RB
Friedelin-3α-ol ***(1)***	428.7	1	1.7	7	20.9	1
Friedelan-3-one ***(2)***	426.7	0	2	6.9	25.9	0
Friedelin-3β-ol ***(3)***	428.7	1	1	7	2.9	1
2β,6β,21α-Trihydroxyfriedelan-3-one ***(4)***	460.7	3	7.1	3.8	84.9	3
3β-Acetyl tormentic acid ***(5)***	530.7	3	6	5.4	104.6	4
Arjunolic acid ***(6)***	488.7	4	7.1	4.2	99.6	5
N-*Benzoyl-L-phenylalaninyl*-N-*benzoyl-L-phenylalaninate* ***(7)***	506.6	2	6	6	104.8	11
Betulinic acid ***(8)***	456.7	2	3.7	6.2	58.3	3
Sitosterol-3β-*O*-D-glucopyranoside ***(9)***	576.9	4	10.2	4.9	97.1	13
N-trans-*p-Coumaroyltyramine* ***(10)***	283.3	3	4	2.7	83.8	8
Known Ligands						
Glucose 6-phosphate (G6P)	260.1	6	18.5	−3.7	154.2	8
16-Bromodehydroepiandrosterone (16BrDHEA)	367.3	1	3.7	3.8	46.5	1
16-Bromoepiandrosterone (16BrEA)	369.3	1	3.7	3.7	43.4	1
Cholesterol	386.7	1	1.7	6.9	21.9	6
Dehydroepiandrosterone (DHEA)	288.4	1	3.7	3.3	46.6	1
Epiandrosterone (EA)	290.4	1	3.7	3.5	44.6	1

MW =Molecule weight; HBD = Hydrogen bond donor; HBA = Hydrogen bond acceptor; PSA = Polar Surface Area; RB = Rotatable Bonds.

4. Conclusion

In this study, a previously unreported triterpenoid, 2β,6β,21α-trihydroxyfriedelan-3-one (**4**) has been isolated from the stems and roots of *D. albidum.* The known 3β-acetyl tormentic and arjunolic acids were obtained for the first time from the genus. The occurrence of friedelan-3α-ol is rare and reported herein for the first time from a *Dichapetalum* species. The isolation of the new compound, another six known triterpenoids and a dipeptide, as well as the absence of dichapetalins from the plant may be important from a chemotaxonomic perspective. The activities of friedelan-3α-ol (**1**) against *S. aureus*, friedelan-3-one (**2**) against *B. cereus*, 3β-acetyl tormentic acid (**5**), against *T. b. brucei*, and sitosterol-3β-*O*-D-glucopyranoside (**9**) against *L. donovani* together indicate the antimicrobial activities of these constituents. The molecular docking into the active site of glucose-6-phosphate dehydrogenase (G6PDH), together with the experimental biological activities against *T. b. brucei* and *L. donovani* parasites, suggest that 3β-acetyl tormentic acid (**5**) and sitosterol-3β-*O*-D-glucopyranoside (**9**) are worth considering for optimization as drug leads.

Author contribution statement

Mary Anti Chama, Ph.D: Conceived and designed the experiments; Performed the experiments; Analyzed and interpreted the data; Contributed reagents, materials, analysis tools or data; Wrote the paper.

Godwin A. Dziwornu, Ph.D: Conceived and designed the experiments; Performed the experiments; Analyzed and interpreted the data; Wrote the paper.

Elizabeth Popli, MPhil: Performed the experiments.

Eduard Mas-Claret, Ph.D: Analyzed and interpreted the data; Contributed reagents, materials, analysis tools or data; Wrote the paper.

Beverly Egyir, Ph.D: Conceived and designed the experiments; Analyzed and interpreted the data; Contributed reagents, materials, analysis tools or data.

Daniel M. Ayine-Tora, Ph.D; David G. Reid, Ph.D; Melinda Duer: Analyzed and interpreted the data; Contributed reagents, materials, analysis tools or data.

Kofi B-A. Owusu, Ph.D: Performed the experiments; Analyzed and interpreted the data.

Dorcas Osei-Safo, Ph.D; Andreas Bender, Ph.D: Conceived and designed the experiments; Analyzed and interpreted the data; Contributed reagents, materials, analysis tools or data.

Dulcie Mulholland, Ph.D: Conceived and designed the experiments; Analyzed and interpreted the data; Contributed reagents, materials, analysis tools or data; Wrote the paper.

Data availability statement

Data included in article/supp. material/referenced in article.

Funding

This work was supported by Alborada Research Grant [Grant Number RG86330] and Isaac Newton Matching Fund [Grant Number 17.07(c)].

Declaration of competing interest

The authors declare that they have no known competing financial interests or personal relationships that could have appeared to influence the work reported in this paper.

Acknowledgement

We are grateful to the Department of Chemistry, University of Ghana and the Yusuf Hamied Department of Chemistry, University of Cambridge for Nuclear Magnetic Resonance and Mass spectral analyses. We are also grateful to the University of Auckland for the modelling work.

Appendix A. Supplementary data

Supplementary data to this article can be found online at https://doi.org/10.1016/j.heliyon.2023.e18299.

References

[1] W.M. Bandaranayake, Quality control, screening, toxicity, and regulation of herbal drugs, in: I. Ahmad, F. Aqil, M. Owais (Eds.), Modern Phytomedicine: Turning Medicinal Plants into Drugs, Wiley-VCH, Verlag GmbH & Co. KGaA, Weinheim, 2006, pp. 25–57.
[2] F.W. Muregi, A. Ishih, T. Miyase, T. Suzuki, H. Kino, T. Amano, G.M. Mkoji, M. Terada, Antimalarial activity of methanolic extracts from plants used in Kenyan ethnomedicine and their interactions with chloroquine (CQ) against a CQ-tolerant rodent parasite, in mice, J. Ethnopharmacol. 111 (1) (2007) 190–195, https://doi.org/10.1016/j.jep.2006.11.009.
[3] P. Amoa Onguéné, F. Ntie-Kang, L.L. Lifongo, J.C. Ndom, W. Sippl, L.M. Mbaze, The potential of anti-malarial compounds derived from African medicinal plants. Part I: a pharmacological evaluation of alkaloids and terpenoids, Malar. J. 12 (1) (2013) 449, https://doi.org/10.1186/1475-2875-12-449.
[4] H. Achenbach, S.A. Asunka, R. Waibel, I. Addae-Mensah, I.V. Oppong, Dichapetalin A, A Novel plant constituent from Dichapetalum madagascariense with potential antineoplastic activity, Nat. Prod. Lett. 7 (2) (1995) 93–100, https://doi.org/10.1080/10575639508043195.
[5] I. Addae-Mensah, R. Waibel, S.A. Asunka, I.V. Oppong, H. Achenbach, The dichapetalins-A new class of triterpenoids, Phytochemistry 43 (3) (1996) 649–656, https://doi.org/10.1016/0031-9422(96)00350-0.
[6] D. Osei-safo, M.A. Chama, I. Addae-Mensah, R. Waibel, W.A. Asomaning, I.V. Oppong, Dichapetalin M from Dichapetalum madagascariensis, Phytochem. Lett. 1 (2008) 147–150.
[7] C. Long, Y. Aussagues, N. Molinier, L. Marcourt, L. Vendier, A. Samson, V. Poughon, P.B. Chalo, F. Ausseil, F. Sautel, et al., Dichapetalins from Dichapetalum species and their cytotoxic properties, Phytochemistry 94 (2013) 184–191.
[8] S.-X. Jing, S.-H. Luo, C.-H. Li, J. Hua, Y.-L. Wang, X.-M. Niu, X.-N. Li, Y. Liu, C.-S. Huang, Y. Wang, et al., Biologically active dichapetalins from Dichapetalum gelonioides, J. Nat. Prod. 77 (2014) 882–893.
[9] M.A. Chama, G.A. Dziwornu, R. Waibel, D. Osei-Safo, I. Addae-Mensah, J. Otchere, M. Wilson, Isolation, characterization, and anthelminthic activities of a novel dichapetalin and other constituents of Dichapetalum filicaule, Pharm. Biol. 54 (7) (2015) 1179–1188.
[10] D. Osei-Safo, G.A. Dziwornu, A. Salgado, S.N. Sunassee, M.A. Chama, Bi- and bisbibenzyls from the roots of Dichapetalum heudelotii and their antiproliferative activities, Fitoterapia 122 (2017) 95–100.
[11] D-l Zhang, M. Li, W.-F. Xu, H. Yu, P.-F. Jin, S.-Y. Li, S.-A. Tang, Nine new dichapetalin-type triterpenoids from the twigs of Dichapetalum, Fitoterapia 151 (2021), 104868.
[12] B. Zhou, X.H. Gao, M.M. Zhang, C.Y. Zheng, H.C. Liu, J.M. Yue, Discovery of four modified classes of triterpenoids delineated a metabolic cascade: compound characterization and biomimetic synthesis, Chem. Sci. 2 (28) (2021) 9831–9838.
[13] P. Tuchinda, J. Kornsakulkarn, M. Pohmakotr, P. Kongsaeree, S. Prabpai, C. Yoosook, J. Kasisit, C. Napaswad, S. Sophasan, V. Reutrakul, Dichapetalin-type triterpenoids and lignans from the aerial parts of Phyllanthus acutissima, J. Nat. Prod. 71 (4) (2008) 655–663.
[14] Bull Soc Bot France 59 (1912) 645–646.
[15] M.A. Chama, B. Egyir, K. Owusu, , B-A, M. Ohashi, Phytochemical composition and in vitro antibacterial activities of Millettia chrysophylla and Millettia zechiana, JUST 40 (1) (2022) 66–85, https://doi.org/10.4314/just.v40i1.1263.
[16] M.A. Chama, D. Modos, L.H. Mervin, K.B.-A. Owusu, D.M. Ayine-Tora, B. Egyir, L. Paemka, G. Yankson, M. Ohashi, A.M. Afzal, A. Bender, Towards understanding antimicrobial activity, cytotoxicity, and the mode of action of dichapetalins A and M using in silico and in vitro studies, Toxicon 193 (2021) 28–37, https://doi.org/10.1016/j.toxicon.2021.01.002.
[17] L. Luzzatto, G. Battistuzzi, Glucose-6-phosphate Dehydrogenase: Advances in Human Genetics 14. Boston (MA), Springer, 1985, pp. 217–329.
[18] M. Scott, L. Zuo, B. Lubin, D. Chiu, NADPH, not glutathione, status modulates oxidant sensitivity in normal and glucose-6-phosphate dehydrogenase-deficient erythrocytes, Blood 77 (9) (1991) 2059–2064.
[19] P.P. Pandolfi, F. Sonati, R. Rivi, P. Mason, F. Grosveld, L. Luzzatto, Targeted disruption of the housekeeping gene encoding glucose 6-phosphate dehydrogenase (G6PD): G6PD is dispensable for pentose synthesis but essential for defense against oxidative stress, EMBO J. 14 (21) (1995) 5209–5215.
[20] H. Ho, M. Cheng, D.T. Chiu, Glucose-6-phosphate dehydrogenase from oxidative stress to cellular functions and degenerative diseases, Redox Rep. 12 (3) (2007) 109–118.
[21] S. Gupta, M. Igoillo-Esteve, P.A. Michels, A.T. Cordeiro, Glucose-6-phosphate dehydrogenase of trypanosomatids: characterization, target validation, and drug discovery, Mol Biol Intern. 2011 (2011) 1–10.
[22] A. Cordeiro, O.H. Thiemann, P.A.M. Michels, Inhibition of Trypanosoma brucei glucose-6-phosphate dehydrogenase by human steroids and their effects on the viability of cultured parasites, Bioorg. Med. Chem. 17 (6) (2009) 2483–2489.
[23] A. Cordeiro, O.H. Thiemann, 16-Bromoepiandrosterone, an activator of the mammalian immune system, inhibits glucose 6-phosphate dehydrogenase from Trypanosoma cruzi and is toxic to these parasites grown in culture, Bioorg. Med. Chem. 18 (13) (2010) 4762–4768.
[24] S. Gupta, A.T. Cordeiro, P.A.M. Michels, Glucose-6-phosphate dehydrogenase is the target for the trypanocidal action of human steroids, Mol and Biochem Parasit 176 (2) (2011) 112–115.
[25] G.F. Mercaldi, A.T. Ranzani, A.T. Cordeiro, Discovery of new uncompetitive inhibitors of glucose-6-phosphate dehydrogenase, J. Biomol. Screen 19 (10) (2014) 1362–1371.
[26] G.F. Mercaldi, A. Dawson, W.N. Hunter, A.T. Cordeiro, The structure of a Trypanosoma cruzi glucose-6-phosphate dehydrogenase reveals differences from the mammalian enzyme, FEBS Lett. 590 (2016) 2776–2786.
[27] H.M. Berman, J. Westbrook, Z. Feng, G. Gilliland, T. Bhat, H. Weissig, I.N. Shindyalov, P.E. Bourne, The protein data bank, Nucleic Acids Res. 28 (1) (2000) 235–242.

[28] H. Berman, K. Henrick, H. Nakamura, Announcing the worldwide protein data bank, 980, Nat. Struct. Mol. Biol. 10 (12) (2003) 980.
[29] Scigress: Version FJ 2.6 (EU 3.1.7) Fujitsu Limited 2008-2016.
[30] G. Jones, P. Willett, R.C. Glen, A.R. Leach, R. Taylor, Development and validation of a genetic algorithm for flexible docking, J. Mol. Biol. 267 (3) (1997) 727–748.
[31] M.D. Eldridge, C.W. Murray, T.R. Auton, G.V. Paolini, R.P. Mee, Empirical scoring functions: I. The development of a fast empirical scoring function to estimate the binding affinity of ligands in receptor complexes, J. Comput. Aided Mol. Des. 11 (5) (1997) 425–445.
[32] M.L. Verdonk, J.C. Cole, M.J. Hartshorn, C.W. Murray, R.D. Taylor, Improved protein–ligand docking using gold, Proteins 52 (4) (2003) 609–623.
[33] O. Korb, T. Stutzle, T.E. Exner, Empirical scoring functions for advanced protein− ligand docking with plants, J. Chem. Inf. Model. 49 (1) (2009) 84–96.
[34] W. Mooij, M.L. Verdonk, General and targeted statistical potentials for protein–ligand interactions, Proteins 61 (2) (2005) 272–287.
[35] QikProp, Schrödinger, LLC, New York, NY, 2023.
[36] M. Laing, M.E. Burke-Laing, R. Bartho, C.M.W. 153, Crystal and molecular structure of epifriedelinol, Tetrahedron Lett. 43 (43) (1977) 3839–3842.
[37] K. Kannathasan, A. Senthilkumar, V. Venkatesalu, Crystal structure and antibacterial evaluation of epifriedelinol isolated from Vitex peduncularis Wall. Ex Schauer, Arab. J. Chem. 12 (8) (2019) 2289–2292.
[38] D. Osei-Safo, M.A. Chama, I. Addae-Mensah, R. Waibel, Hispidulin and other constituents of Scoparia dulcis Linn, JUST 29 (2) (2009) 7–15, https://doi.org/10.4314/just.v29i2.46218.
[39] M.A. Chama, H.A. Onyame, C. Fleischer, D. Osei-Safo, R. Waibel, J. Otchere, I. Addae-Mensah, M. Wilson, In vitro activities of crude extracts and triterpenoid constituents of Dichapetalum crassifolium Chodat against clinical isolates of Schistosoma haematobium, Heliyon 6 (7) (2020).
[40] P. Tane, A. Tsopmo, D. Ngnokam, F. Ayafor, O. Sterner, New friedelane triterpenes from Lepidobotrys staudtii, Tetrahedron 52 (47) (1996) 14989–14994.
[41] G.G. Rocha, M. Simões, K.A. Lúcio, R.R. Oliveira, M.A. Coelho Kaplan, C.R. Gattass, Natural triterpenoids from Cecropia lyratiloba are cytotoxic to both sensitive and multidrug resistant leukemia cell lines, Bioorg. Med. Chem. 15 (2007) 7355–7360.
[42] R. Csuk, B. Siewert, C. Dressel, R. Schäfer, Tormentic acid derivatives: synthesis and apoptotic activity, Eur. J. Med. Chem. 56 (2012) 237–245.
[43] A.P. Kundu, S.B. Mahato, Triterpenoids and their glycosides from Terminalia, Chebula Phytochemistry 32 (4) (1993) 999–1002.
[44] J.L. Songue, Dongo E. Kouam, T.N. Mpondo, R.L. White, Chemical constituents from stem bark and roots of Clausena anisata, Molecules 17 (11) (2012) 13673–13686.
[45] J.J. Bankeu, S.A. Mustafa, A.S. Gojayev, B.D. Lenta, D. Tchamo Noungoué, S.A. Ngouela, K. Asaad, M.I. Choudhary, S. Prigge, A.A. Guliyev, et al., Ceramide and Cerebroside from the stem bark of Ficus mucuso (Moraceae), Chem. Pharm. Bull. (Tokyo) 58 (12) (2010) 1661–1665.
[46] I. Addae-Mensah, S. Adu-Kumi, R. Waibel, I.V. Oppong, A novel D: a-friedooleanane triterpenoid and other constituents of the stem bark of, Dichapetalum barteri Engl. Arkivoc 1 (9) (2007) 71–79.
[47] M.A. Chama, A.M. Appiah, S. Gbewonyo, V.F. Darbah, D. Osei-Safo, R. Waibel, J. Otchere, M. Wilson, I. Addae-Mensah, Evaluation of Insecticidal, anti-hookworm activities of crude extracts and isolates from Dichapetalum madagascariense stem bark, JUST 37 (3) (2017) 54–66.
[48] G.O. Okafor, A.O. Oyewale, J. Habila, J. Akpemi, Isolation, characterization , and assessment of the in vitro antibacterial and antifungal properties of methanol extracts and friedelan-3-one from Uapaca ambanjensis (Leandri), M. A, J. Appl. Sci. Environ. Manag. (26) (2022) 1479–1486.
[49] I.C. Odeh, T.A. Tor-anyiin, J.O. Igoli, J.V. Anyam, In vitro antimicrobial properties of friedelan-3-one from Pterocarpus santalinoides L ' Herit , ex Dc, African Journal of Biiotechnology 15 (14) (2016) 531–538, https://doi.org/10.5897/AJB2015.15091.
[50] F. Zhu, G. Logan, J. Reynisson, Wine compounds as a source for HTS screening collections. A feasibility study, Mol Inf 31 (11–12) (2012) 847–855.